

AERODYNAMIC FEATURES OF A COAXIAL ROTOR HELICOPTER

V.A. ANIKIN

Kamov Helicopter Scientific & Technology Company

USSR

Abstract

The paper presents the coaxial - rotor helicopter aerodynamic features. The influence of the induced interaction of the rotors on the rotor system aerodynamics in hover and forward flight is shown, which is compared with the equivalent single rotor characteristics. The influence of the coaxial rotors aerodynamic symmetry on the helicopter vibration and trim characteristics is addressed. The coaxial rotor aerodynamic features at the gliding mode and unsteady flapping characteristics of a blade are described. The coaxial type helicopter fuselage layout features are presented. The paper discusses the numerical simulation problems of the coaxial helicopter aerodynamics and its elements.

Nomenclature

η	- rotor system efficiency,
σ	- rotor solidity
K_A	- number of blades
N	- required power
C_y	- lift coefficient, $C_y = \frac{Y}{\rho/2 (\omega R)^2 \pi R^2}$
C_x	- drag coefficient, $C_x = \frac{X}{\rho/2 (\omega R)^2 \pi R^2}$
V	- flight speed, $\bar{V} = V/\omega R$

- C_T - rotor thrust coefficient, $C_T = \frac{T}{\rho/2 (\omega R)^2 \pi R^2}$
 m_K - rotor torque coefficient $m_K = \frac{M_K}{\rho/2 (\omega R)^2 \pi R^3}$
 a_{1o}, b_{1o} - coefficients of the blade flapping first harmonic
 α - angle of attack
 C_{xa} - aerodynamic drag coefficient, $C_x = \frac{X}{\frac{\rho}{2} V^2 S_m}$
 θ - pitch angle
 δ_z - rotor force resultant angle
 h - minimum coaxial rotor blade spacing, $\bar{h} = h/R$
 ψ_i - blade encountering azimuth angles
 ψ_o - phase angle
 Subscripts
 o - single rotor
 c - coaxial rotor
 B - upper rotor (U.R.)
 H - lower rotor (L.R.)

Coaxial-rotor helicopter aerodynamics features some important peculiarities which make its functional capabilities different from those of other helicopter schemes. Aerodynamics of coaxial helicopter components is analysed and the results are compared with familiar aerodynamic data of a single-rotor helicopter.

1. COAXIAL ROTORS AERODYNAMICS.

Let us examine rotor system aerodynamics of a single-rotor and coaxial-rotor helicopters. We shall compare two coaxial rotors having K_A blades each and a single rotor with $2xK_A$ blades providing they have equal diameters, $2xR$, equal tip velocity, R , and identical blade geometry and profiles.

Airflow over two coaxial, closely-located rotors substantially differs from that over a single rotor due to longitudinal aerodynamic symmetry and inductive coupling between the rotors. The lower is the flight speed, the higher is the influence of the rotor interactional inductance on the aerodynamic characteristics of each rotor and the rotor system itself. In hover the influence of an inductive power component is of primary importance. Fig.1 shows efficiency values of two coaxial rotors and of an equivalent single rotor in hover.

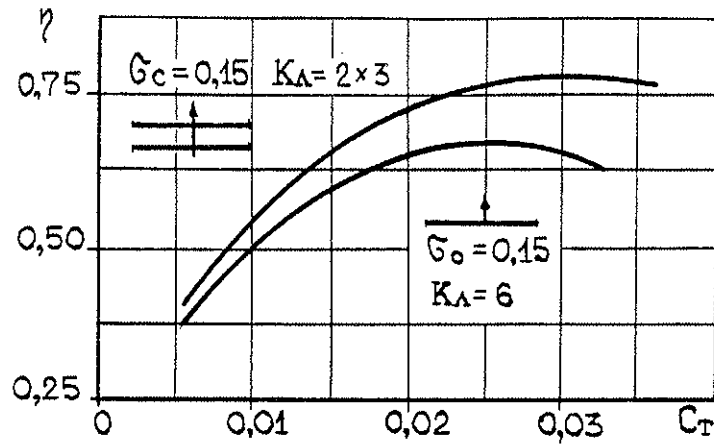


Fig.1 Efficiency of coaxial rotors and an equivalent single rotor.

It is seen that inductive interaction of coaxial rotors has a stronger influence on the lift-to-drag ratio than that of coaxial propellers relative to an equivalent propeller. Higher efficiency of coaxial propellers is achieved mainly by the elimination of a wake swirl behind them and of coaxial rotors - additionally by the wake contraction.

When comparing power characteristics of a single-rotor and coaxial-rotor helicopters at take-off, besides rotor system efficiency differences it is necessary to take account of additional power losses for a tail rotor of a single-rotor helicopter and the specified excess power depending on the take-off conditions. As a result the required hovering power of a coaxial-rotor helicopter is substantially lower than of a single-rotor helicopter which is equivalent to an extra hovering ceiling of 2,000 m. Depending on the take-off requirements such reserve could be greater or less. For example if a helicopter is to perform hovering turns with a constant angular velocity, a single-rotor helicopter needs additional power comparable to power consumption required to counteract main rotor torque in hover without turn. Such additional power wasted for turning practically doesn't exist for a coaxial helicopter. In case when it is necessary to perform a hovering turn by a predetermined angle in a specified time a single-rotor helicopter may achieve higher acceleration due to its tail rotor.

Thus, at take-off regimes a coaxial-rotor helicopter has substantially lower required power in comparison with a single-rotor helicopter. This factor is used to improve flight performance such as to increase hovering ceiling, rate of climb, or to reduce rotor system dimensions, retaining the same flight performance, to achieve some operational advantages.

It is coaxial rotors aerodynamics that defines the helicopter aerodynamic features and flight performance in level flight. As the flight speed increases the influence of the coaxial rotors inductive interaction on aerodynamic characteristics becomes less. Fig.2 shows a comparison of required power of a single and coaxial-rotor helicopters with the same parasite drag values. But to design a coaxial helicopter with low drag is a complicated task because coaxial rotor hubs and intermediate shaft with control rods ("rotor column" structure) are poorly-streamlined bodies. Therefore a coaxial-rotor helicopter has lower required power in level flight than single-rotor helicopter at low and medium flight speeds and higher power - at higher flight speeds. As a consequence, a coaxial-rotor helicopter features good maximum rates of climb, hovering and service ceilings, flight performance with one engine inoperative and prolonged flight. A single-rotor helicopter is characterized by high maximum and cruise speeds and flight range.

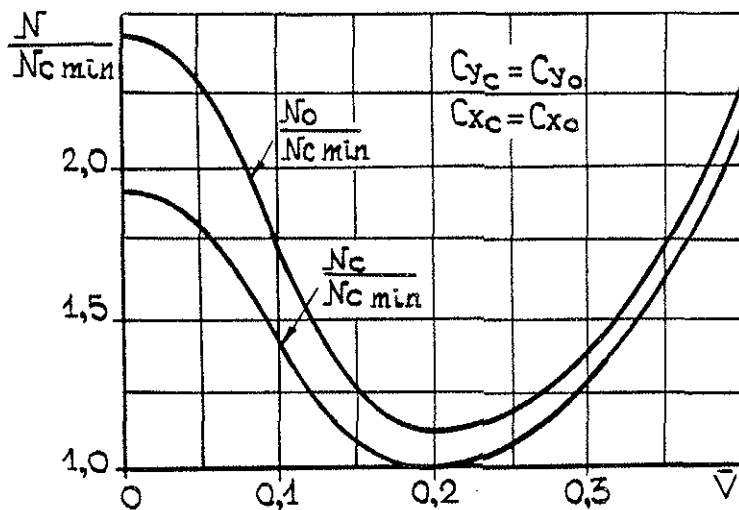


Fig.2 Relative required power of a single-rotor helicopter versus flight speed.

Furthermore to the coaxial rotors power characteristics it is necessary to mention their aerodynamic symmetry. In operation a coaxial-rotor helicopter is devoid of some undesirable peculiarities inherent in a single-rotor helicopter. A coaxial-rotor helicopter is characterized by independent longitudinal and lateral movements, poor control cross-couplings in the entire operational range. These factors allow to unload the pilot, to simplify and to improve flying qualities and to design highly-efficient automated flight control systems.

The helicopter performance in descent are strongly influenced by coaxial rotor aerodynamics. The required power decreases as well as the available rotor torque necessary for directional control. At the same time rotor aerodynamic loads are redistributed. Fig.3 shows the relationship between thrust coefficients of an upper and lower rotors in descent. As seen on the diagram there exist the regimes of deep gliding where the upper rotor "choking" occurs. This phenomenon takes place as a rule beyond the autorotation limit. In descent new peculiarities of aerodynamic characteristics development appear. Extensive experimental and theoretical studies have been undertaken to investigate the revealed unsteady blade flapping motion.

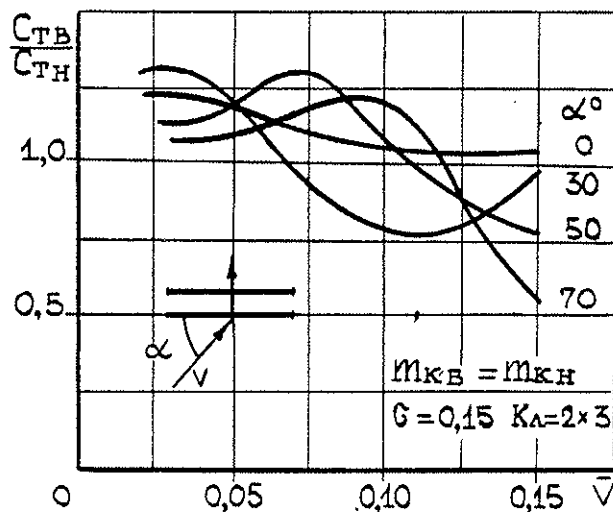


Fig.3 Thrust coefficient ratio of the upper and lower rotors in descent.

In descent phase there are regions where blade flap angle fluctuations could be rather great and blade flapping behaviour changes - the first harmonic decreases and higher harmonics increase due to the motion instability. The region of unsteady motion of a single rotor is substantially larger in comparison with the same region of coaxial rotors (see Fig.4).

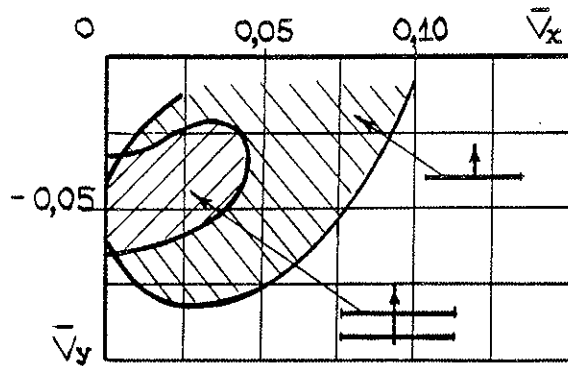


Fig.4 Areas of unsteady flapping motion of single and coaxial rotors.

Another peculiarity of coaxial rotors aerodynamics which is important in operation is the possibility to affect aerodynamic load variations taken up by the fuselage. One can change vibration level of a helicopter airframe by changing the phase angle (ψ_0) of the upper rotor relative to the lower one (Fig.5).

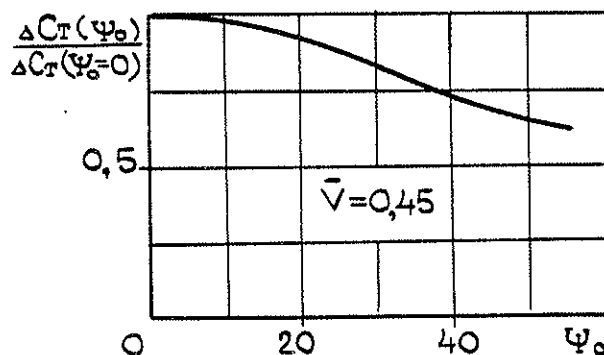


Fig.5 Thrust coefficient amplitude ratio versus rotor phase angle.

Due to the peculiarities of its aerodynamic and weight configurations a coaxial-rotor helicopter is highly maneuverable. It is achieved by moving the aerodynamic force application point (long arms) and low inertia moments (absence of far-separated masses). It results in high control power and acceleration values for a coaxial helicopter. For example, time to achieve the predetermined pitch angle is twice less as compared with an equivalent single-rotor helicopter. In-heading maneuvering and, particularly, descent maneuvering is not efficient. It is explained by power drop and control moments decrease. Therefore rudders are fitted on coaxial-rotor helicopters to increase the control moments in heading during descent.

Approaching processes of the blades of the upper and lower rotors in level flight and during spatial maneuvering have been investigated in detail. The nature of such approaching process is defined by blade aerodynamics and flexibility characteristics as well as by "rotors column" kinematics. In some cases the linkages flexibility of the coaxial rotors and the column contributes to the process. The blades approach each other at encountering azimuth angles when the upper rotor blade passes over the lower one. For three-bladed coaxial rotors there are six azimuth angles. Rotor spacing and kinematic behaviour of the rotor control system are chosen such as to maximize the minimum rotor spacing in the entire design range. Blade approaching function of the Ka 32 helicopter in level flight is shown in Fig.6.

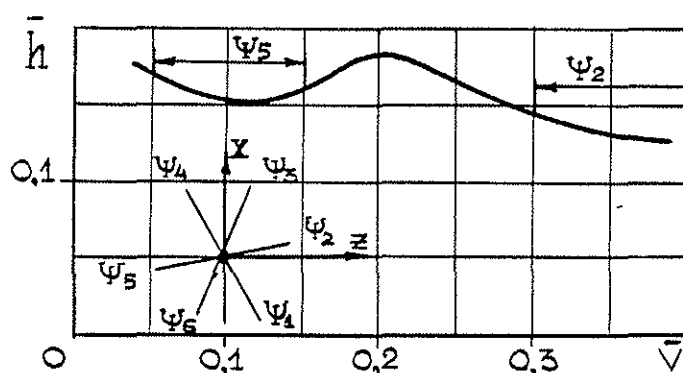


Fig.6 Maximum coaxial rotor blades approach as a function of the speed.

In forward flight the closest approach of the blades occurs leftward (azimuth $\sim 270^\circ$) and as flight speed increases - rightward, in the region of $\sim 90^\circ$.

2. AERODYNAMICS OF COAXIAL-ROTOR HELICOPTER AIRFRAME.

In some past years Kamov Design Bureau has been actively involved in improving the aerodynamic configuration of a helicopter airframe and in raising the flight speed. The results of the studies aimed at designing high-speed coaxial and single-rotor helicopters with low parasite drag are shown in Fig.7. The results revealed that there are good prospects to decrease the existing drag level. For comparison the results of the S-76 helicopter model testing performed by Mr. A. Dyachenko are also shown on this diagram. The results allow to predict maximum flight speed increase of a coaxial helicopter by 50...70 km/h. Two versions of an airframe aerodynamic configuration have been developed. The first one was intended for operation from the sites of limited dimensions and has a fuselage which doesn't extend beyond the rotor disc limit (Ka 15, Ka 26, Ka 32). Moreover, this configuration features high rotor loads and 10...20% smaller diameter in comparison with a similar single-rotor helicopter.

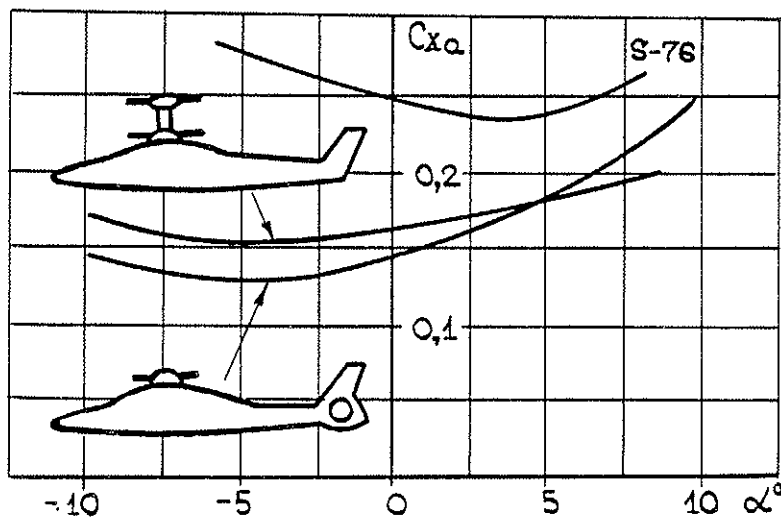


Fig.7 Parasite drag of coaxial helicopter airframes.

Therefore, a coaxial-rotor helicopter has the smallest dimensions among different helicopter schemes. The most difficult element in developing this type of aerodynamic configuration is the empennage. It functions in the aerodynamic shadow of the fuselage body and should ensure helicopter stability in a wide range of angles of attack and slip angles. That is why the empennage has two fins fixed on the tips of a stabilizer which is mounted at a small distance from the center of gravity (0.65 of rotor radius). In case one of the fins gets into the fuselage shadow in slipping motion the second one functions effectively. The stabilizer location helps to eliminate the so called "spoon" phenomenon of longitudinal control in forward flight. Vertical and horizontal tail areas of this coaxial rotor helicopter configuration are evidently larger than those of a single-rotor helicopter. It is accounted for small arms and high airflow deceleration behind the poorly-streamlined fuselage. The described empennage configuration provides for acceptable directional and longitudinal stability parameters at all flight regimes including the descent phase. The limitations of this configuration are additional rotor thrust losses for blowing and higher drag attributed to the angular fins. Pitch angles, \bar{U} , and rotor force resultant angles, δ_z , of the Ka 32 helicopter in forward and rearward flights are shown in Fig.8.

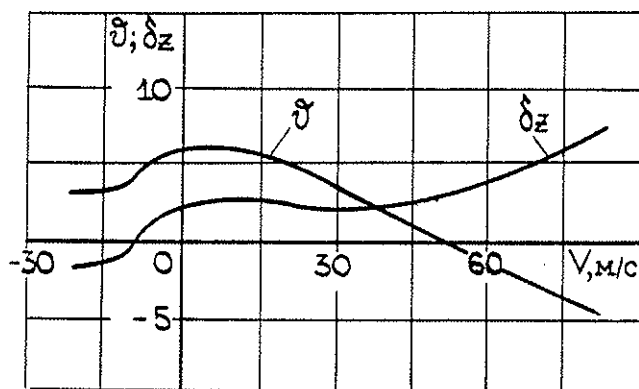


Fig.8 Trim characteristics of a coaxial rotor helicopter.

As evident from Fig.8, trim non-linearities in rearward flight caused by rotors vortex interference with the empennage don't complicate piloting technique.

Another empennage configuration for coaxial helicopters has been developed which extends beyond the coaxial rotor disc. It comprises a fin and a stabilizer mounted on it. Such a configuration allows to decrease power losses for blowing, to improve empennage operating conditions, to eliminate "spoon" phenomenon in trim functions and to decrease power losses in horizontal flight caused by the empennage negative lift.

3. MATHEMATICAL SIMULATION PECULIARITIES.

Aerodynamic simulation problems are the same for coaxial and single rotors [1]. The main difference is the necessity to simulate rotors inductive interactions and the interference between one rotor vortex and the other rotor blades. To calculate flight performance and trim characteristics of a coaxial-rotor helicopter various mathematical models are used with different degrees of detail. A linear vortex theory of coaxial rotors is developed to carry out parametric study and to select the helicopter parameters. This theory postulates the transition from a variety of helical vortex filaments to vortex layers (disc vortex theory). It allows to solve rigorously the problem of deriving hydrodynamic peculiarities of rotor-rotor vortex interaction and creating a model of inductive interaction of coaxial rotors characterized by low computer power cost. Based on the same model it is possible to describe rather accurately the aerodynamic characteristics of the airframe in the rotors velocity field using inductive washes near the airframe components.

Let us describe the rotor vortex model (Fig.9). The rotor blades are schematically shown as radial vortex segments.

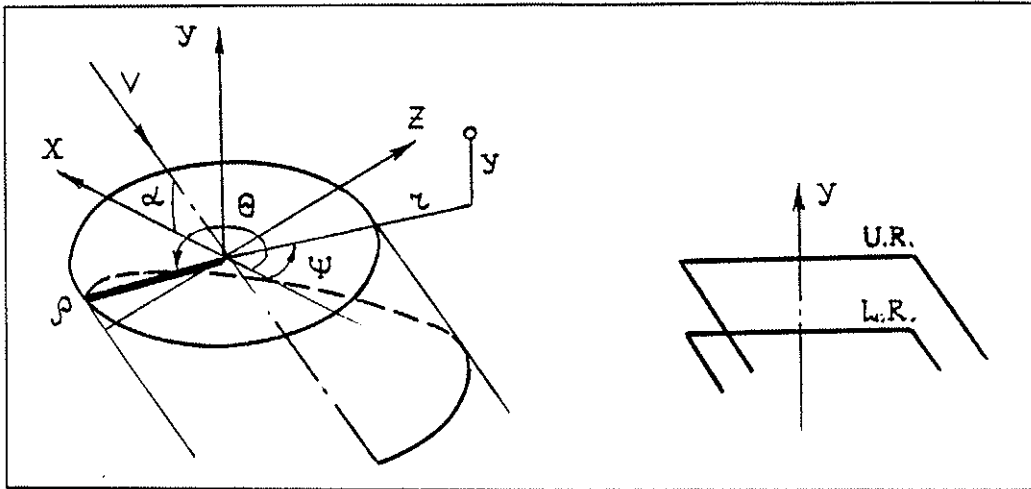


Fig.9 Rotor vortex model.

Continuous vortex layer running off the blades at V velocity generates a skewed helical surface with a constant pitch extending to infinity. Vortex column axis makes an α angle with X axis. If vortex surface equation and the polar system coordinates of the point where the inductive velocity is defined, are substituted into Biot - Savart's equation, linear dimensions are related to rotor radius, velocity values - to blade tip velocity, ωR , and circulation - to ωR^2 , after transition to vortex layers we get:

$$\bar{U}_a = \frac{\kappa_1}{4\pi V} \int_0^{2\pi} \frac{d\bar{r}}{d\bar{\rho}} I^a(\bar{\rho}, \bar{z}, \bar{y}, \psi, \bar{v}, \alpha) d\bar{\rho},$$

$$I^x = \frac{1}{2\pi} \int_0^{2\pi} \frac{\bar{\rho} \cos \theta (L \sin \alpha - \bar{y}) + \bar{v} L_z \sin \alpha}{L(L^* + L_x \cos \alpha)} d\theta,$$

$$I^y = \frac{1}{2\pi} \int_0^{2\pi} \frac{\bar{\rho} \cos \theta \cos \alpha}{L^* + L_x \cos \alpha} + \frac{\bar{\rho}^2 - \bar{\rho} \bar{z} \cos(\theta - \psi) + \bar{v} L_z \cos \alpha}{L(L^* + L_x \cos \alpha)} d\theta$$

$$I^z = \frac{1}{2\pi} \int_0^{2\pi} \frac{-\bar{\rho} \sin \theta (L \sin \alpha - \bar{y}) + \bar{v} (\bar{y} \cos \alpha + L_x \cos \alpha)}{L(L^* + L_x \cos \alpha)} d\theta$$

$$L = \sqrt{\bar{y}^2 + \bar{z}^2}, \quad l = \sqrt{\bar{\rho}^2 + \bar{z}^2 - 2\bar{\rho}\bar{z}\cos(\theta - \psi)}, \quad L^* = L - \bar{y}\sin \alpha$$

$$L_x = \bar{\rho} \cos \theta - \bar{z} \cos \psi, \quad L_z = \bar{\rho} \sin \theta - \bar{z} \sin \psi.$$

A hypothesis of circulation azimuth regularity is used in the above formulae when applied to coaxial rotors with their longitudinal symmetry. In predicting upper rotor inductive velocity in the plane of the lower rotor there are a number of peculiarities in the integrands. To extract them the velocity components are presented as Fourier series, particularly for "y" component.

$$\bar{v}_y(\bar{z}, \bar{y}, \psi) = \bar{v}_e^y(\bar{z}, \bar{y}) + \sum_{n=1}^{\infty} [\bar{v}_{cn}^y(\bar{z}, \bar{y}) \cos n\psi + \bar{v}_{sn}^y(\bar{z}, \bar{y}) \sin n\psi],$$

where

$$\bar{v}_p = \frac{K_1}{4\pi V} \int_0^1 \frac{d\bar{r}}{d\bar{\rho}} I_p^y d\bar{\rho}, \quad p = e, p = cn, p = sn.$$

There are formulae for coefficients:

$$I_e^y = \frac{1}{\pi} \int_0^\pi \frac{\bar{\rho}^2 - \bar{\rho}\bar{z} \cos \theta}{\rho^2} \left(1 + \frac{j\bar{y}}{L}\right) d\theta; \quad I_{sn}^y = \frac{(-1)^{n+1}}{\pi} \cdot 2\bar{y} \int_0^\pi \frac{\cos n\varphi}{L} W_n d\theta,$$

$$I_{cn}^y = (-1)^n \frac{2}{\pi} \int_0^\pi \left(\frac{j\bar{y}}{L} \cdot \frac{\bar{\rho}^2 - \bar{\rho}\bar{z} \cos \theta}{\rho^2} \cdot \cos n\varphi - \bar{z} \frac{\sin \varphi \sin n\varphi}{\rho} \right) W_n d\theta,$$

$$\sin \varphi = \frac{\bar{\rho} \sin \theta}{\rho}, \quad \cos \varphi = \frac{\bar{\rho}\bar{z} \cos \theta - \bar{z}}{\rho},$$

$$W_n = \left[\frac{L}{\rho} \left(1 + \frac{j\bar{y}}{L}\right) \frac{\cos \alpha}{1 + j \sin \alpha} \right]^n, \quad j = \begin{cases} 1, & L \sin \alpha > \bar{y} \\ -1, & L \sin \alpha \leq \bar{y} \end{cases}$$

When $y \sin \alpha \leq 0$

$$W_n = W_n(\bar{\rho}, \bar{z}, \bar{y}, \theta) \cdot k^n(\alpha)$$

Where k

$$k(\alpha) = \frac{\cos \alpha}{1 + |\sin \alpha|}$$

Function $j(\bar{\rho}, \bar{z}, \bar{y}, \alpha, \theta)$ analytically describes the extracted peculiarity after integration. In the smooth region this function identically equals ± 1 and in the vortex layer region it changes the sign after integration with respect to preserving its limitation. The above formulae allow to describe the velocity field induced by the rotor vortex at a random point in space. They could be presented as a combination of elliptical integrals of three forms and algebraic functions. The system of integro-differential equations of coaxial rotors relative to circulations (which correspond to constant azimuth portion of the thrust distributed along blade radius) consists of well-known expressions for angle of attack of a blade section which accounts for additional inductive velocity generated by the neighbouring rotor.

The system solution is sought after it is transformed to a system of algebraic equations by numerical procedures.

For hover, non-linearity components are to be taken into account in the coaxial rotors vortex structure. Corrections for wake contraction behind the rotors and for vortex drift velocity variations over the vortex column height are also introduced. In view of this vortex column is subdivided into zones. The wake is considered to be cylindrical and the velocity - constant over the elementary zone height.

Aerodynamic characteristics of coaxial rotors are predicted by numerically integrating blade motion with respect to familiar relationships of a single rotor theory [1,2]. Each rotor functions in the field of additional inductive velocities induced by the neighbouring rotor. It gives rise to the redistribution of blade section angles of attack and aerodynamic loads.

Fig.10 shows first harmonic coefficients of the upper/lower blade flapping motion in simultaneous operation and at the distance as a function the flight speed.

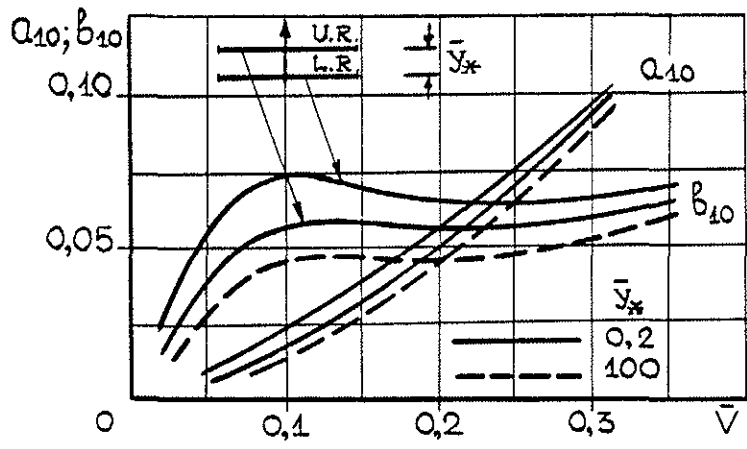


Fig.10 First harmonic coefficient of coaxial rotor blade flapping motion.

Prediction of coaxial rotors aerodynamic characteristics based on the above model makes it possible to describe flight performance and trim characteristics of a coaxial-rotor helicopter with acceptable degree of accuracy. The aerodynamic characteristics of the airframe with installed rotors are defined from results of model wind tunnel testing with allowance for inductive washes based on a disc model. Simulation results of the fuselage longitudinal moment with the rotor and without it are presented in Fig.11.

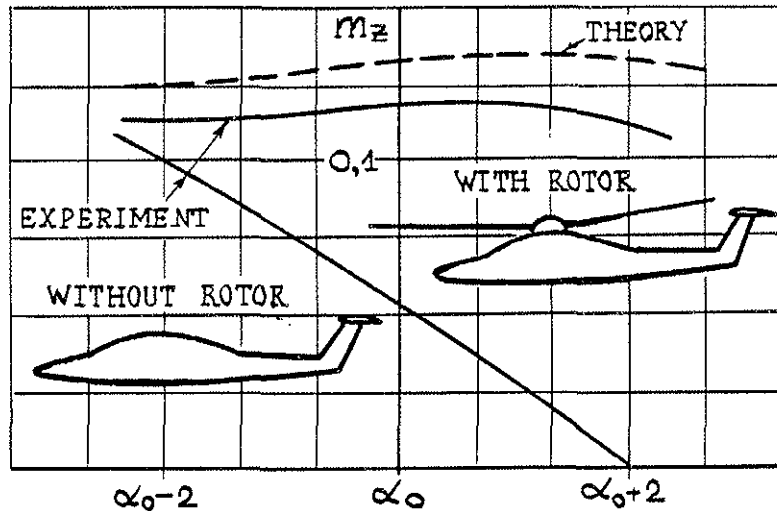


Fig.11 Rotor influence on a longitudinal moment of a fuselage with empennage.

The above model is satisfactory for describing vortex-airframe interaction in sideward flight where the inductive influence factors are significant.

To simulate blade aerodynamics a non-linear vortex theory is developed. Blade S_0 is represented by a lifting surface S with free vortex surfaces \mathcal{S} running off it. For disturbed velocity potential Laplace equation $\nabla^2 \varphi = 0$ holds true, the condition of the absence of flow through the lifting surface normal to it (\vec{n}) , $(\nabla \varphi - \vec{w}) \vec{n} = 0$, $(x, y, z) \in S$

Free vortex sheet satisfies the condition of pressure continuity $p_+ = p_-$ and normal velocity component $(\nabla \varphi \vec{n})_+ = (\nabla \varphi \vec{n})_-$ where subscripts "+" and "-" correspond to different surface sides. At infinity the fluid is at rest.

The task of φ potential definition under given boundary conditions has a non-linear nature. Substitution of a continuous distributed vortex layer with a discrete one in accordance with discrete vortex method makes it possible to change from integro-differential equations to a system of algebraic ones. Boundary conditions for the absence of flow through the lifting surface in a given number of points as well as Chaplygin-Zhukovsky hypothesis for sharp edges allow to write the solving system of equations relative to unknown circulations of attached vortices at each time instant.

Sampling and schematic presentation are given in Fig.12.

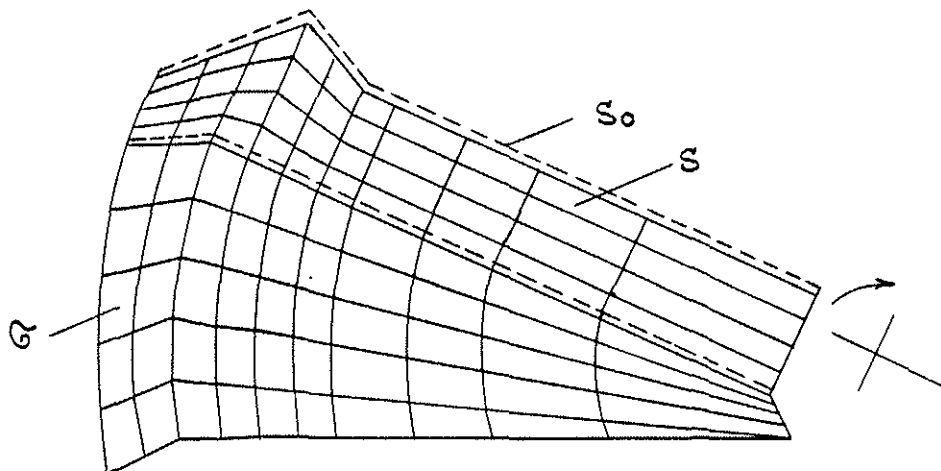


Fig.12 Blade vortex structure scheme.

The trajectory of free vortices is determined by time step solution of differential equations.

$$\frac{d\xi}{dt} = w_x - w_x^* \quad ; \quad \frac{d\eta}{dt} = w_y - w_y^* ;$$

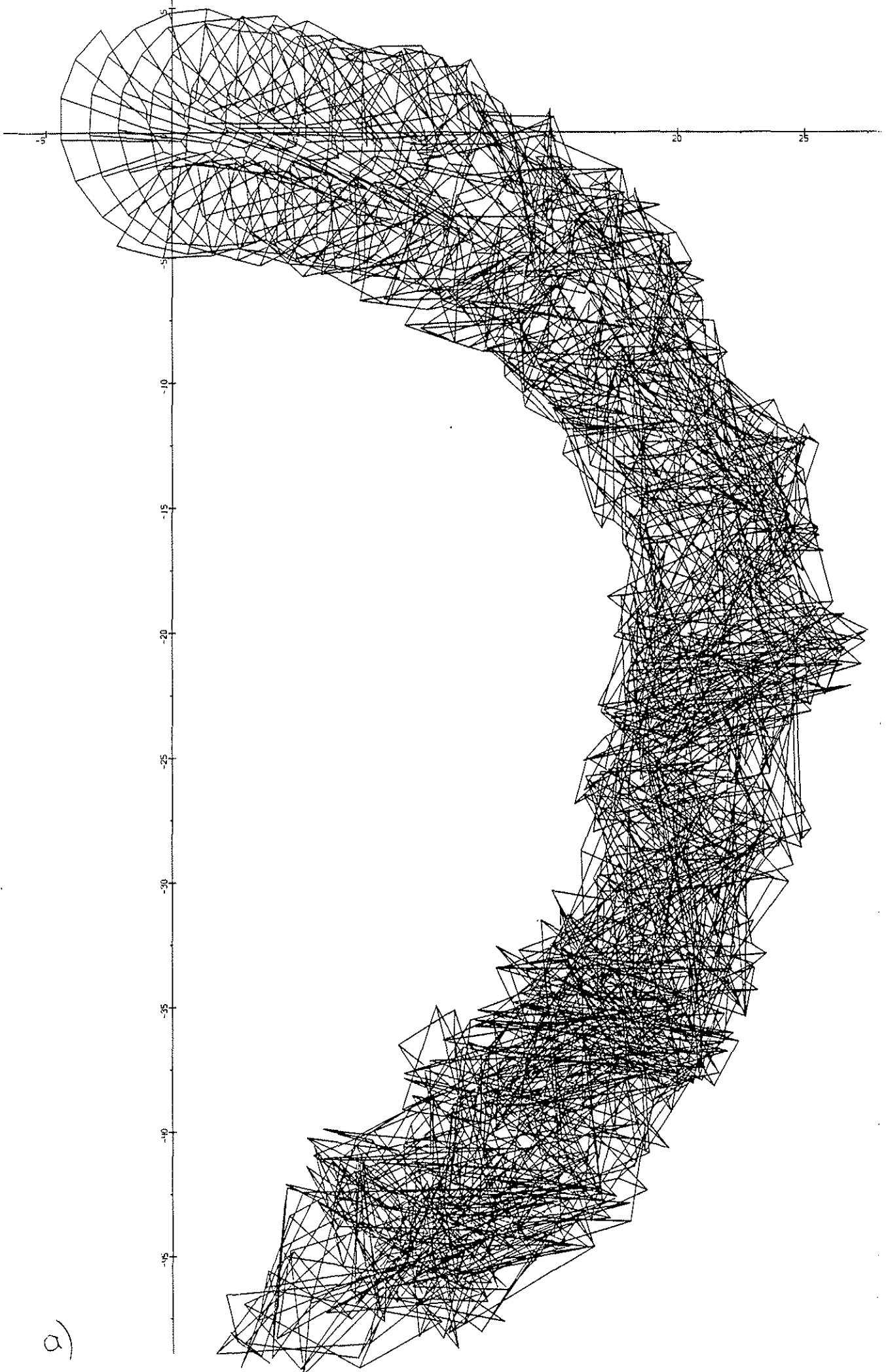
$$\frac{d\xi}{dt} = w_z - w_z^*$$

where $\{\xi, \eta, \xi\}$ - are vortex coordinates, $\vec{w}^* = \vec{v} + \vec{\omega} * \vec{r}$ - transfer velocity, \vec{w} - disturbance velocity.

Section aerodynamic load is determined by Cauchy-Lagrange integral [3].

Drag forces as well as the influence of compressibility and viscosity are predicted using experimental data of profile wind-tunnel testing. Flapping motion equations integrate to blade flapping characteristics.

A rotor vortex structure in spatial maneuvering, represented by a downgoing spiral is shown in Fig.13 (a - top view, b - rear view).



a)

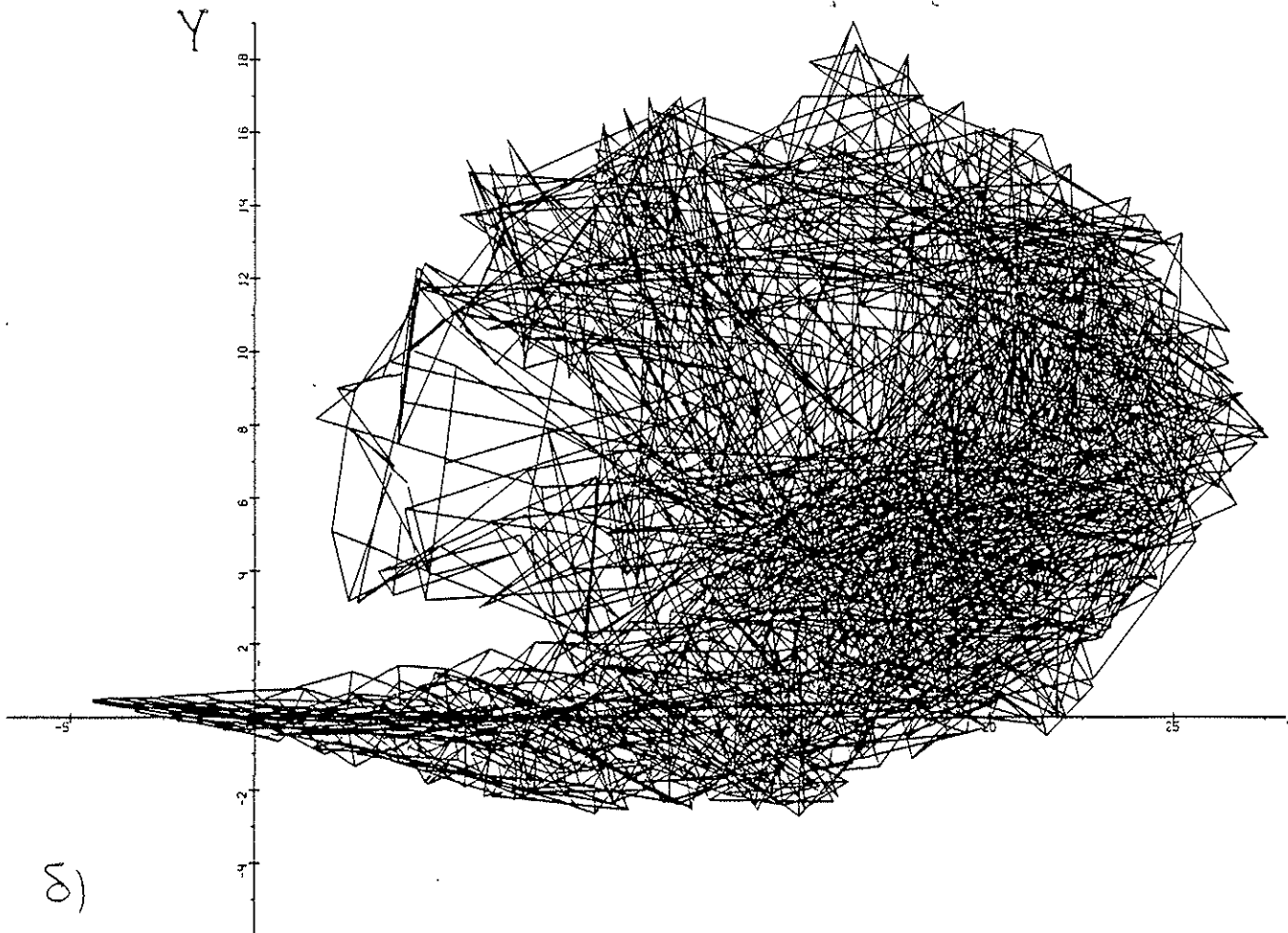


Fig.13 Coaxial rotor vortex wake during helicopter spatial maneuvering.

Fig.14 shows velocity field of coaxial rotors in longitudinal section $z=0$ for steep descent at $\alpha=50^\circ$. Illustrative diagram showing the effect of a blade tip shape on thrust-coefficient-to-rotor-power-coefficient ratio and on the semiswing amplitude of the pitch moment $\pm M_{\omega}$ at angle of attack $\alpha=0$, without flapping motion at $V=0.5$ is given in Fig.15.

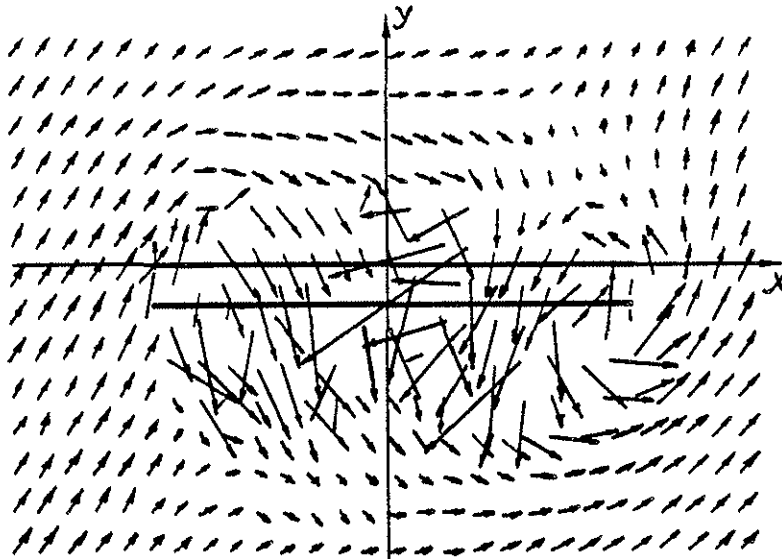


Fig.14 Velocity field near rotors in descent.

The above described non-linear vortex theory of the rotors allows to simulate unsteady flapping motion of coaxial rotor in descent.

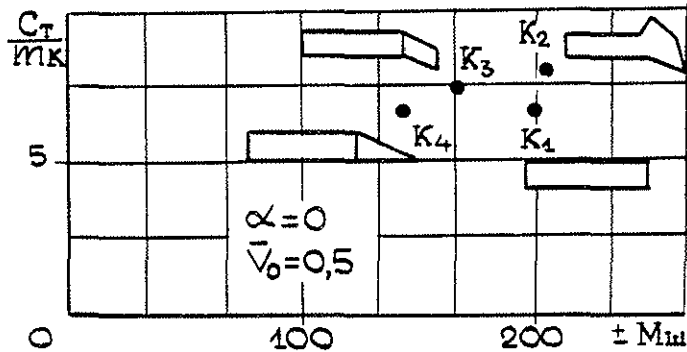


Fig.15 Influence of blade tip shapes on rotor aerodynamics.

Within the vortex model various degrees of detail are assumed. In practice several model versions have been developed with a blade representation simplified to a vortex filament or with simplified description of a free vortex surface at a specified distance from the rotor.

Vortex-blade interaction is modeled using "thick" vortices. Namely, based on the blade scheme a vortex diameter is determined which equals half length of the smallest elementary panel. Vortex induced velocity is limited and changes linearly from the vortex boundary to zero along its axis. Thus mathematic peculiarities are eliminated during vortex structures interaction.

Based on the developed vortex models of coaxial rotors, helicopter movement models are created with different degree of detail of rotor aerodynamics, models of the flexible blades motion and approach during helicopter spatial maneuvering and some others which allow to describe aerodynamic peculiarities of coaxial rotors and the helicopter.

References

1. V.E.Baskin, L.S.Vildgrube, E.S.Vozhdaev, G.I.Maykapar "Theory of a lifting rotor", Moscow, "Mashinostroenie", 1973.
2. M.L.Mil, A.V.Nekrasov, A.S.Braverman, L.N.Grodko, M.A.Leykand "Helicopters", v.1, Moscow, "Mashinostroenie", 1966.
3. S.M.Belotserkovsky, V.A.Vasin, B.E.Loktev "Development of unsteady non-linear theory of an air screw", "Izvestija of the USSR Academy of science", 1975, No.5.